Mass transport generated by stratified internal wave boundary layers

Conference Paper · June 2017

3 authors, including:

Ernesto Horne
Ecole Centrale de Lyon

Leo R Maas
Utrecht University

Mass transport generated by stratified internal wave boundary layers

F. Beckebanze[1], E. Horne Iribarne[2], and L.R.M. Maas[3]

[1]Mathematical Institute, Utrecht University, Netherlands
Email: f.beckebanze@uu.nl
[2]Ecole Centrale de Lyon, Université de Lyon, France
[3]Institute for Marine and Atmospheric research Utrecht, Utrecht University, Netherlands

Keywords: internal waves, induced mean flow, stratified boundary layers, mass transport.

Abstract

Internal waves, generated by tidal oscillations over rough bottom topography at the margins of shallow seas, are known to be important for the mixing budget of the ocean. One of the open questions in the dynamics of the ocean is related to mechanisms by which energy is transferred to smaller scales, where mixing takes place. Using small-amplitude expansions, we investigate the mass transport generated by monochromatic internal wave beams between two lateral boundaries in the laminar regime. We find that the peculiar 3D structure of the lateral viscous boundary layers results in effective Reynolds stresses near the lateral walls, which generates a horizontal circulation in the interior. This induced circulation increase linearly over time, and as such, it may lead to the onset of wave-mean flow interactions and to turbulent mixing. Surprisingly, even very thin boundary layers ($\sim 1\%$ of wall to wall distance) have a significant impact on the mass transport in the interior. The theory is verified by laboratory experiments on particle transport induced by quasi-2D internal wave beams.

1. Introduction

It is well known that turbulent mixing by time-periodic internal wave beams (IWBs) plays an important role in stirring the oceans, especially in shallow marginal seas (Wunsch and Ferrari, 2004). Relatively little attention has been paid to the laminar regime, in which IWBs can also modify the oceanic background state.
We study the impact of IWBs on the background by constructing small-amplitude expansions under idealized settings. For this we consider monochromatic quasi-2D IWBs between two lateral walls. Recently, it has been recognized that the energy dissipation of quasi-2D IWBs in the laboratory can only be understood when taking the lateral boundary layers into account (Beckebanze and Maas, 2016).
In this study, we compute the mass transport generated through Reynolds forcing in the lateral boundary layers (§4). The Reynolds stresses by quasi-2D IWBs, which is negligible in the interior, induces a mean flow near the lateral walls, which in turn drives a horizontal return flow through the interior. The return flow is in opposite direction relative to the horizontal IWB energy propagation direction, and increases linearly over time, which agrees well with laboratory experiments by Hazewinkel, (2010, §7) and Horne Iribarne (2015, §5).
This mass transport mechanism might be relevant to sediment and nutrient transport in the marginal seas, at the border of which internal waves tend to be generated (Egbert and Ray, 2001). It may also lead to the onset of turbulent mixing through wave-mean flow interactions in otherwise laminar regimes.
In §4 we compare our theory with laboratory experiments by Horne Iribarne (2015), and conclusions are drawn in §5.

2. Preliminaries

We study monochromatic internal waves with frequency ω_0 in a linearly stratified Boussinesq fluid. We consider Cartesian coordinates (x,y,z) between two lateral walls at $y = \pm l_y$, with z anti-parallel to gravity, g, see Fig. 1a. The equations governing the dimensionless velocity field $\mathbf{u} = (u,v,w)$, buoyancy b, and pressure p of the Boussinesq fluid, employing scaled Brunt-Väisälä frequency $N = N_0/\omega_0 = \pm 1/\sin\theta$, are given in subscript-derivative notation by

$$\mathbf{u}_t + \varepsilon\,\mathbf{u}\cdot\nabla\mathbf{u} = -\nabla p + \delta^2\Delta\mathbf{u} + b\hat{z}, \qquad b_t + \varepsilon\,\mathbf{u}\cdot\nabla b = -N^2 w, \qquad \nabla\cdot\mathbf{u} = 0. \tag{1}$$

Here, $\delta = \frac{d_0}{L_0} \ll 1$ is the thickness of the Stokes boundary layer, $d_0 = \sqrt{\nu/\omega_0}$, scaled cross-beam wave length, L_0. The Stokes number, $\varepsilon = \frac{U_0}{\omega_0 L_0}$, with U_0 the dimensional scale of the velocity vector $\mathbf{u} \in \mathscr{O}(1)$, is also assumed to be small. We solve (1) under no-slip boundary conditions, $\mathbf{u} = \mathbf{0}$ at the lateral walls, $y = \pm l_y$, by expanding the velocity vector $\mathbf{u}$ in the small parameter δ, and using the slow time-scale $T = \varepsilon t$,

$$\mathbf{u}(t) = \Re\left[\mathbf{u}_0\exp[-it] + \delta\mathbf{u}_1\exp[-it] + \bar{\mathbf{u}}_0(T)\right] + \mathscr{O}(\delta\varepsilon),$$

and similarly for buoyancy b and pressure p. Here, the overbar denotes the component which varies only slowly in time, i.e. $\partial_t\bar{\mathbf{u}}_0 \in \mathscr{O}(\varepsilon)$. Beckebanze and Maas (2016) found the following asymptotic solutions to the linearized system (1):

$$\begin{aligned}
&u_0 = \cos\theta\,(1-E[y])\,U(\zeta), && b_0 = \tfrac{-i}{\sin\theta}\,(1-E^*[y\cot\theta)]\,U(\zeta),\\
&v_1 = \left(i\sin\theta\cos\theta\left(\tan^2\theta\;E'^*[y\cot\theta] + E'[y]\right) + y\,l_y^{-1}\sin\theta e^{-i(\sigma+\pi/4)}\right)U'(\zeta), && p_0 = -i\cot\theta\;U(\zeta),\\
&w_0 = -\sin\theta\,(1-E^*[y\cot\theta])\,U(\zeta), && E[y] = \frac{\cosh[i^{-\frac{1}{2}}\delta^{-1}y]}{\cosh[i^{-\frac{1}{2}}\delta^{-1}l_y]},
\end{aligned} \tag{2}$$

with $*$ denoting complex conjugate, $'$ derivative, and U is the velocity component in the along-beam direction, $\xi = x\cos\theta - z\sin\theta$. The phase propagation is upwards along $\zeta = x\sin\theta + z\cos\theta$, normal to ξ, see Fig. 1a. For the comparison with the laboratory experiments described below, we choose $U = \exp[ik_0\zeta]$ for $t \geq 0$ and $|\zeta| < 2L_0$ (with $k_0 = 2\pi/L_0$) and $U = 0$ else wise. This instantaneous appearance of the wave beam at $t = 0$ may be used for the Reynolds stresses generating the mean velocity field, $\bar{\mathbf{u}}_0$ (with $\bar{\mathbf{u}}_0 = \mathbf{0}$ at $t = 0$), provided that $\bar{\mathbf{u}}_0$ evolves slowly over time, i.e. if $\varepsilon \ll 1$. In general, one may also consider viscous IWBs for velocity field U, such as described by Thomas and Stevenson (1973).

3. Induced horizontal circulation

In the current study, we find that the induced mean velocity field may be described by $\bar{\mathbf{u}}_0 = (\bar{\Psi}_y, -\bar{\Psi}_x, 0)$, because $\bar{w}_0$, which is fixed by the time-independent part of the buoyancy advection, $\varepsilon\,\mathbf{u}_0\cdot\nabla b_0$, is $\mathscr{O}(\varepsilon)$ (small) at all times T. The stream function $\bar{\Psi}$ for the induced horizontal circulation is then governed by the vertical vorticity equation at $\mathscr{O}(\varepsilon)$,

$$\partial_T\Delta\bar{\Psi} = \Im[UU_\zeta^*]\partial_y F(y), \quad \text{for } T > 0 \qquad \text{with} \qquad \bar{\Psi} = 0 \text{ at } y = \pm l_y \text{ and at } T = 0 \tag{3}$$

with the spatial structure of the Reynolds stresses - determined by the solutions (2) to the linearization of (1) - given by

$$\begin{aligned}
F(y) = &\frac{\cos^2\theta\sin\theta}{2}\left(G[|y|-l_y] + G[\cot\theta(|y|-l_y)] + (\tan\theta - 1)G[(1+\cot\theta)(|y|-l_y)]\right)\\
&+\frac{\cos\theta\sin\theta}{2}e^{\frac{|y|-l_y}{\sqrt{2}\delta}}\left(\cos\left[\theta + \frac{|y|-l_y}{\sqrt{2}\delta}\right] - \cos\theta e^{\frac{|y|-l_y}{\sqrt{2}\delta}}\right) + \mathscr{O}(\delta l_y^{-1}),
\end{aligned}$$

with $G[y] := \exp\left[\frac{y}{\sqrt{2}\delta}\right]\sin\left[\frac{y}{\sqrt{2}\delta}\right]$. Interestingly, not only the two length scales of vertical and horizontal boundary layer, respectively $\delta\cot\theta$ and δ, but also their sum, $\delta(1+\cot\theta)$, appears in the spatial structure of the Reynolds stresses, $F(y)$. Fig. 1b presents $\bar{u}_0 = \bar{\Psi}_y$ at $t = 2\pi$ for the parameter values corresponding to the laboratory experiment described below. The exact expression for $\bar{u}_0$, which is omitted due to its extend, is $\mathscr{O}(T)$ near the lateral walls and $\mathscr{O}(T\delta l_y^{-1}(1+\cot\theta))$ in the interior (respectively red and blue areas in Fig. 1b). For sufficiently large T, the (Eulerian) induced mean circulation, $\bar{\mathbf{u}}_0$, (which increases linearly over time T) is much larger than the Stokes Drift (independent of T), such that $\bar{\mathbf{u}}_0$ also describes the net mass transport (mean Lagrangian velocity).

4. Laboratory experiments

In a series of laboratory experiments, described in more detail in §5 in Horne Iribane (2015), IWBs are generated by a wave maker inside a rectangular tank with dimensions $80\times 17\times 42$ cm^3 (L x W x H). The wave maker, located at one side of the tank ($x = 0$), generates a wave beam with frequency $\omega_0 = 0.25$ rad/s, wave length $L_0 = 3.7$ cm and cross-beam width of $4L_0$, propagating downwards at an angle $\theta = 0.22$ rad with respect to the horizontal (Fig. 1c).

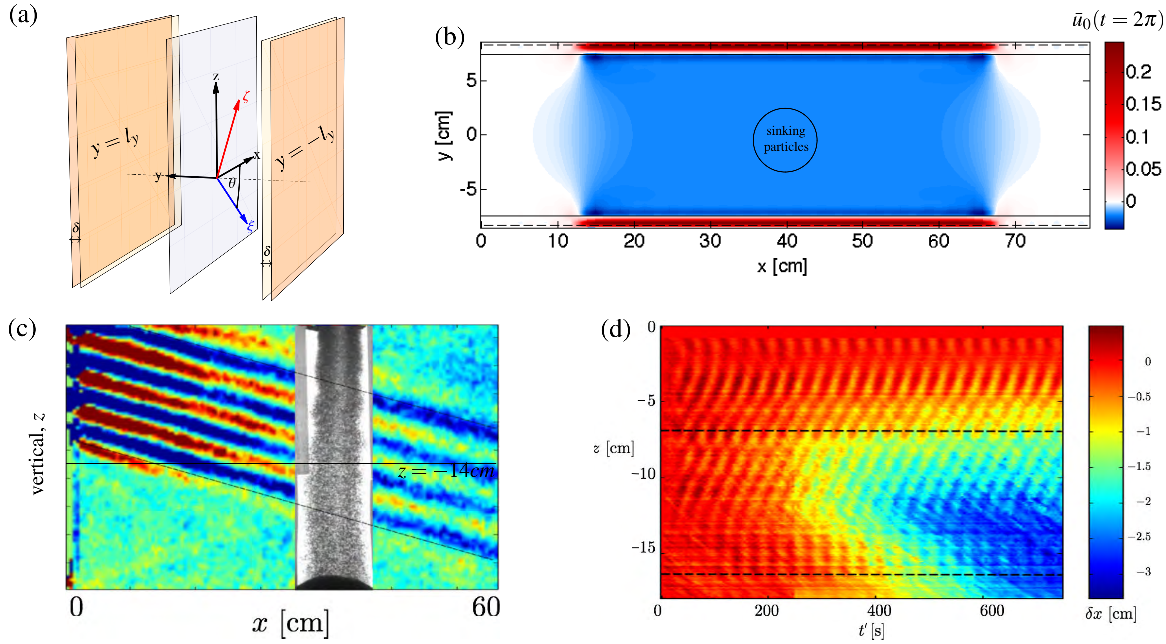

Figure 1: (a) Sketch of the 3D infinite domain between two lateral walls at $y = \pm l_y$, and (b) top view (aspect ratio = 1) of the induced mean horizontal along-wall flow, $\bar{u}_0$, in the horizontal plane $z = -14$ cm, for parameter values corresponding to the experimental set-up. The two thin lateral boundary layers (width $d_0 = 2$ mm, indicated by dashed lines) are much smaller than the region with thickness $(1+\cot\theta)d_0$ over which the Reynolds stresses are significant (solid lines). The circle indicates the position of the sinking particles in the corresponding experiment. (c) The side view of the laboratory set-up shows the wave beam, generated at $x = 0$ cm, which intersects the sinking particles (gray column) at $x \approx 40$ cm. (d) The contours indicate the observed horizontal particle displacements as a function of time and vertical position, z. The two horizontal dashed lines indicate the positions where the wave beam passes through the column.

Particles of a controlled size are released into the fluid at approximately 40 cm from the wave maker (in x-direction, gray column in Fig. 1c). The sedimentation velocity of the particles is 0.9 mm/s, which means that it takes about six wave periods ($12\pi/\omega_0 \approx 150$ s) to sink through the wave beam. Our theory predicts that the dimensionalized induced horizontal mean velocity field, $U_0\bar{\mathbf{u}}_0$, transports the sinking particles in the horizontal direction. At the particle column ($x \approx 40$ cm) the observed wave beam velocity amplitude is $U_0 = 0.9$ mm/s (implying $\varepsilon = 0.1$). The theoretical horizontal displacement of the particles leaving the wave beam at time t' (in seconds) is determined from the solution to (3) as $\delta x(t') = U_0 \int_{-12\pi/\omega_0+t'}^{t'} \bar{u}_0(\tau/\omega_0)d\tau \approx 0.1t' - 7.5$ mm for $t' > 150$ s (6 periods). Fig. 1d presents the observed horizontal displacement of the column of particles as a function time and vertical position, indicating that the particle displacement increases indeed linearly over time. Note that the particles leaving the wave beam at the end of the experiment ($t' = 750$ s) are horizontally displace by 6.7 cm theoretically, whereas in the experiment we find 3.5 cm.

5. Discussion and Conclusions

The present analysis establishes the importance of the lateral boundary layers on the mass transport induced by IWBs. We find that the net mass transport, which is confined to horizontal planes due to the presence of stratification, increases linearly over time on intermediate time scales determined by the Stokes number, ε. Over sufficiently long time periods, two scenarios are possible: (1) Saturation of the induced velocity field, in a balance with viscous dissipation or (2) nonlinear wave-mean flow interactions, which may lead to turbulent mixing.

References

Beckebanze, F. & Maas, L.R.M. (2016) Damping of 3D internal wave attractors by lateral walls, *Conf. proc. of VIIIth ISSF*.
Egbert, G. D. & Ray, R. D. (2001) Estimates of M2 tidal energy dissipation from TOPEX/Poseidon altimeter data, *J. of Geophy. Research*, Vol. 106, 22475 -22502.
Hazewinkel, J. (2010) Attractors in stratified fluids, PhD thesis, ISBN: 978-90-9025020-5.
Horne Iribarne, E. (2015) Transport properties of internal gravity waves, PhD thesis.
Thomas, N.H. & Stevenson, T.N. (1973) An internal wave in a viscous ocean stratified by both salt and heat. *J. Fluid Mech.*, Vol. 61, 301-304.
Wunsch, C. & Ferrari, R. (2004) Vertical mixing, energy, and the general circulation of the oceans. *Annu. Rev. Fluid Mech.*, Vol. 36, 281-314.